HHS Public Access

Author manuscript

Neuroscience. Author manuscript; available in PMC 2020 August 21.

Published in final edited form as:

Neuroscience. 2019 August 21; 414: 88–98. doi:10.1016/j.neuroscience.2019.06.039.

GPR55-mediated effects on brain microvascular endothelial cells and the blood-brain barrier

Luciana M. Leo[1], **Boluwatife Familusi**[2], **Michelle Hoang**[2], **Raymond Smith**[2], **Kristen Lindenau**[2], **Kevin T. Sporici**[2], **Eugen Brailoiu**[1], **Mary E. Abood**[1], **G. Cristina Brailoiu**[2,*]

[1]Center for Substance Abuse Research, Lewis Katz School of Medicine, Philadelphia, PA 19140

[2]Department of Pharmaceutical Sciences, Jefferson College of Pharmacy, Philadelphia, PA 19107

Abstract

GPR55, an atypical cannabinoid receptor activated by lysophosphatidylinositol (LPI) has been involved in various physiological and pathological processes. We examined the effect of GPR55 activation on rat brain microvascular endothelial cells (RBMVEC), an essential component of the blood-brain barrier (BBB). GPR55 was detected in RBMVEC by western blot and immunocytochemistry. Treatment of RBMVEC with LPI increased cytosolic Ca^{2+} concentration, $[Ca^{2+}]_i$, in a concentration-dependent manner; the effect was abolished by the GPR55 antagonist, ML-193. Repetitive application of LPI induced tachyphylaxis. LPI-induced increase in $[Ca^{2+}]_i$ was not sensitive to U-73122, a phospholipase C inhibitor, but was abolished by the blockade of voltage-gated Ca^{2+} channels or in Ca^{2+}-free saline, indicating that Ca^{2+} influx was involved in this response. LPI induced a biphasic change in RBMVEC membrane potential: a fast depolarization followed by a long-lasting hyperpolarization. The hyperpolarization phase was prevented by apamin and charibdotoxin, inhibitors of small- and intermediate-conductance Ca^{2+}- activated K^+ channels (K_{Ca}). Immunofluorescence studies indicate that LPI produced transient changes in tight and adherens junctions proteins and F-actin stress fibers. LPI decreased the electrical resistance of RBMVEC monolayer assessed with Electric Cell-Substrate Impedance Sensing (ECIS) in a dose-dependent manner. *In vivo* studies indicate that systemic administration of LPI increased the permeability of the BBB, assessed with Evans Blue method. Taken together, our results indicate that GPR55 activation modulates the function of endothelial cells of brain microvessels, produces a transient reduction in endothelial barrier function and increases BBB permeability.

Keywords

blood-brain barrier; calcium signaling; electrical resistance; LPI

[*]Address correspondence to G.C. Brailoiu, M.D., Department of Pharmaceutical Sciences, Jefferson College of Pharmacy, 901 Walnut St, Suite 901, Philadelphia, PA 19107, Phone: 215-503-7468; Gabriela.Brailoiu@jefferson.edu.

Introduction

GPR55 was identified as an atypical cannabinoid receptor, distinct from CB_1 and CB_2 receptors (Baker et al., 2006), whose endogenous ligand is lysophosphatidylinositol (LPI) (Oka et al., 2007). GPR55 is highly expressed in the central nervous system and peripheral organs, in a variety of tissues and cell types, including endothelial cells from different vascular beds (Ryberg et al., 2007, Henstridge et al., 2011, AlSuleimani and Hiley, 2015, Kremshofer et al., 2015). LPI is synthesized from membrane lipids in the presence of phospholipase A2 (Pineiro and Falasca, 2012). Previous studies indicate that endothelial cells produce LPI (Martin and Wysolmerski, 1987, Bondarenko et al., 2010). In addition, an autocrine role for LPI via GPR55 activation was reported in other systems (Pineiro et al., 2011).

Emerging evidence supports the involvement of GPR55 in diverse physiological functions such as synaptic transmission, neuronal development, bone metabolism, glucose metabolism, intestinal motility, vascular function, as well as in pathophysiological states, such as anxiety, pain, inflammation, obesity and cancer (Henstridge et al., 2011, Ross, 2011, Yu et al., 2013, AlSuleimani and Hiley, 2015, Deliu et al., 2015, Guy et al., 2015, Kremshofer et al., 2015, Rahimi et al., 2015, Alhouayek et al., 2018, Ferro et al., 2018, Hill et al., 2018). GPR55 couples with various G-proteins, for example G_q, $G_{12}/_{13}$; downstream signaling mechanisms include PLC and RhoA activation, Ca^{2+} release and ERK1/2 phosphorylation (Ross, 2009, Pertwee et al., 2010, Sharir and Abood, 2010).

GPR55 was identified in microvascular endothelial cells from human dermis (Zhang et al., 2010) and lung (Kargl et al., 2013) where the receptor was involved in endothelial proliferation and wound healing. GPR55 is expressed in human brain microvascular endothelial cells (Hasko et al., 2014) and in hCMEC/D3 endothelial cell line (Al Suleimani and Hiley, 2016). Our study investigated the *in vitro* effects of LPI via GPR55 activation in rat brain microvascular endothelial cells and *in vivo* effects on the blood-brain barrier (BBB) permeability.

Experimental Procedures

Ethical approval

Animal protocols were approved by the Institutional Animal Care and Use Committee from each institution. Adult male Sprague Dawley rats (Charles River Laboratories, Wilmington, MA) were used for *in vivo* studies.

Chemicals and reagents

Soy lysophosphatidylinositol (LPI) was purchased from Avanti Polar Lipids (Alabaster, AL). ML-193 (CID 1261822), N-[4-[[(3,4-dimethyl-5-isoxazolyl)amino]sulfony]-phenyl]-6,8-dimethyl-2-(2-pyridinyl)-4-quinoline-carboxamide was from Cayman Chemicals (Ann Arbor, MI). U-73122 was from Tocris Bioscience (Bio-Techne, Minneapolis, MN). LPI and ML-193 were dissolved in DMSO (stock concentration of 10 mM) and dissolved in Hanks Balanced Salt Solution (HBSS) just before administration. The final concentration of DMSO

(0.1% v/v) did not affect $[Ca^{2+}]_i$. Other reagents were from Sigma-Aldrich (St. Louis, MO) unless otherwise mentioned.

Cell Culture

Rat brain microvascular endothelial cells (RBMVEC) from Cell Applications, Inc (San Diego, CA) were cultured in Rat Brain Endothelial Basal Medium and Rat Brain Endothelial Growth supplement, according to the manufacturer's instructions (Brailoiu et al., 2016, Brailoiu et al., 2017, Brailoiu et al., 2018). Cells were grown in T75 flasks coated with attachment factor (Cell Applications, Inc) until 80% confluent. Cells were plated on round coverslips of 12 mm diameter (immunocytochemistry studies), or 25 mm diameter (live imaging studies), coated with human fibronectin (Discovery Labware, Bedford, MA). For impedance measurements, cells were grown on 8W10E+ arrays (Applied BioPhysics, Inc., Troy, NY) coated with fibronectin, as previously reported (Brailoiu et al., 2018).

Western Blot analysis

Whole-cell lysates of RBMVEC and rat cerebral cortex were separated on Mini-PROTEAN TGX 4–20% gels (Bio-Rad, Hercules, CA) by SDS-PAGE followed by immunoblotting as previously described (Altmann et al., 2015, Brailoiu et al., 2016). Proteins were transferred to an Odyssey nitrocellulose membrane (LI-COR Biosciences, Lincoln, NE). After incubation with blocking buffer, membranes were incubated overnight with primary antibody against GPR55 (rabbit polyclonal against the N-terminus of rat GPR55 (1:1000, cat # ADI-905-900; Enzo Life Sciences, Inc., Farmingdale, NY). An antibody against β-actin (mouse monoclonal, 1:10,000; cat # A5441, Sigma-Aldrich) was used to confirm equal protein loading. Membranes were washed with Tris-buffered saline-Tween 20 (TBST) and incubated with the secondary antibodies: IRDye 800CW conjugated goat anti-rabbit IgG (1:10,000, Cat # 926-32211, LI-COR) and IRDye 680 conjugated goat anti-mouse IgG (1:10,000, Cat # 926-32220, LI-COR) for 1 h at room temperature. Membranes were then washed in TBST and scanned using a LI-COR Odyssey Infrared Imager. Densitometric analysis was performed using Odyssey V.3 software (LI-COR).

Cytosolic Ca^{2+} imaging

Measurements of intracellular Ca^{2+} concentration, $[Ca^{2+}]_i$, were performed as previously described (Brailoiu et al., 2017, Brailoiu et al., 2018). Briefly, cells were incubated with 5 μM Fura-2 AM (Molecular Probes, Life Technologies, Grand Island, NY) in HBSS at room temperature for one hour and washed with dye-free HBSS. Coverslips were mounted in an open bath chamber (QR-40LP, Warner Instruments, Hamden, CT) on the stage of an inverted microscope Nikon Eclipse TiE (Nikon Inc., Melville, NY), equipped with a Photometrics CoolSnap HQ2 CCD camera (Photometrics, Tucson, AZ). Fura-2 AM fluorescence (emission 510 nm), following alternate excitation at 340 and 380 nm, was acquired at a frequency of 0.25 Hz. Images were acquired/analyzed using NIS-Elements AR software (Nikon) and the ratio of the fluorescence signals (340/380 nm) was converted to Ca^{2+} concentrations (Grynkiewicz et al., 1985).

Measurement of membrane potential

RBMVEC membrane potential changes were evaluated in cells loaded with bis-(1,3-dibutylbarbituric acid)-trimethine-oxonol, $DiBAC_4(3)$ (0.5 μM, 30 min), a voltage-sensitive dye, as reported (Brailoiu et al., 2018). The fluorescence (excitation/emission 480nm/540nm) was monitored at 0.1 Hz. Membrane hyperpolarization produces a decrease in fluorescence intensity, whereas depolarization is associated with an increase in the fluorescence intensity due to sequestration of the dye into cytosol (Brauner et al., 1984).

Immunocytochemistry

Immunocytochemistry studies were performed as previously described (Brailoiu et al., 2017, Brailoiu et al., 2018). RBMVEC grown on 12 mm diameter glass coverslips, were treated with LPI (10 μM, 10 min) and processed for immunocytochemistry immediately after treatment or after 1 hour; untreated cells served as control. After rinsing with phosphate buffer saline (PBS), cells were fixed in 4% paraformaldehyde, rinsed with PBS and PBS with 0.5% Triton X for 5 min, and incubated with normal goat serum (1:20, 1 hour, room temperature). Cells were then incubated overnight at 4°C, with the following primary antibody: ZO-1 (1:200, rabbit polyclonal, cat # 40-2200, Thermo Fisher Scientific, Rockford, IL), occludin (1:200, rabbit polyclonal, cat # 71-1500, Thermo Fisher Scientific), VE-Cadherin (1:200, rabbit polyclonal, cat # 36-1900, Thermo Fisher Scientific) followed by incubation with secondary antibody Alexa Fluor 488 goat anti-rabbit IgG (1:200, cat # A11008, Invitrogen, Thermo Fisher Scientific) or Alexa Fluor 568 goat anti-rabbit IgG (1:200, cat # A11011, Invitrogen, Thermo Fisher Scientific) for 2 hours at room temperature. In another series of experiments, cells were washed in PBS and incubated with ActinRed 555 for 30 min, at room temperature. To characterize the distribution of GPR55 in RBMVEC, cells were fixed in 4% paraformaldehyde, rinsed with PBS and PBS with 0.5% Triton X for 5 min, blocked with normal goat serum (1:20, 1 hour, room temperature) and incubated with GPR55 antibody (1:500, rabbit polyclonal, 2 hours, room temperature; a gift from Ken Mackie's Lab) (Korchynska et al., 2019) followed by incubation with secondary antibody Alexa Fluor 488 goat anti-rabbit IgG (1:200, 2 hours, room temperature). In control immunostaining experiments, RBMVEC were processed similarly, but GPR55 antibody was incubated with the GPR55 immunizing peptide (a gift from Ken Mackie's Lab) or the primary (GPR55) antibody omitted. After washing in PBS, cells were mounted with DAPI Fluoromount G (SouthernBiotech, Birmingham, AL), sealed, and examined under a Leica DMI6000B fluorescence microscope equipped with the appropriate filter sets.

Impedance Measurements

Electric cell-substrate impedance sensing (ECIS) method, using a Zθ controller, an 16W array holder station and gold electrode arrays type 8W10E+, was used for impedance measurements, as previously reported (Stolwijk et al., 2015, Brailoiu et al., 2018). RBMVEC (100,000 cells/cm^2) were cultured on 8W10E+ arrays, consisting of 40 gold electrodes for each of the 8 × 0.8 cm^2 wells. Arrays were coated with fibronectin (50μg/ml, 200 μl/well, 30 min, 37°C) and L-cysteine (10 mM, 200 μl/well, 20 min, room temperature). Cells were grown on arrays for 3-4 days in an incubator (37°C, 5% CO_2, humidified atmosphere) and transferred to FBS-free medium before drug treatment. To assess the effect

of LPI on barrier function, the resistance of RBMVEC at 4000 Hz frequency (Giaever and Keese, 1984, Stolwijk et al., 2015), averaged for the cells grown on 40 electrodes/well, was normalized to the value before the addition of the compound and plotted as function of time.

Evans Blue extravasation method

In vivo assessment of BBB disruption was carried out using Evans Blue method, as reported earlier (Uyama et al., 1988, Brailoiu et al., 2018). Evans Blue (2% in PBS; 4 mg/Kg, i.v. via tail vein) was administered 30 min before the i.v injection (via tail vein) of GPR55 ligands. One hour later, rats were anesthetized with ketamine (100 mg/kg) and xylazine (5mg/kg) and perfused transcardially with PBS. After dissection, the brain was weighed and homogenized in PBS, then treated with trichloroacetic acid (80%, 1 hour, 4 °C). After centrifugation (20 min, 10,000 × g), the absorbance (610 nm) of the supernatant was determined using a plate reader (Synergy2, BioTek Instruments, Inc., Winooski, VT) and the brain concentration of Evans Blue determined.

Statistical analysis

Data were expressed as mean ± standard error of mean (SEM). One-way ANOVA followed by post hoc analysis using Bonferroni test was used to evaluate significant differences between groups; two-sample T-Test was used when comparing two different groups; $P < 0.05$ was considered statistically significant.

Results

GPR55 expression and distribution in RBMVEC

Western blot analysis of the whole-cell lysate prepared from RBMVEC identified expression of GPR55 at the protein level (Fig.1A). Rat cerebral cortex, in which we previously identified GPR55 expression (Yu et al., 2013, Deliu et al., 2015) was used as a positive control. Using a GPR55 antibody (Korchynska et al., 2019) we found that in RBMVEC GPR55-like immunoreactivity was present mostly intracellularly; reduced immunoreactivity was detected at the plasma membrane (Fig. 1B-C). In control experiments, where GPR55 antibody was incubated with the GPR55 immunizing peptide (Fig. 1D), or the primary antibody was omitted (Fig. 1E), a low basal fluorescence level was detected.

GPR55 activation increases cytosolic Ca^{2+} concentration, $[Ca^{2+}]_i$, in RBMVEC

Treatment of RBMVEC with LPI (10 μM) induced a fast increase in Fura-2 AM 340/380 fluorescence ratio and $[Ca^{2+}]_i$ (Fig. 2A, B). In cells pretreated with the GPR55 antagonist, ML-193 (10 μM) (Heynen-Genel et al., 2010b, Kotsikorou et al., 2013), LPI (10 μM) did not increase the fluorescence ratio and $[Ca^{2+}]_i$, respectively (Fig. 2A, B). Representative examples of changes in Fura-2 AM 340/380 fluorescence ratio in RBMVEC in response to LPI in the absence and presence of GPR55 antagonist ML-193 are shown in Fig. 2A, and Ca^{2+} traces are shown in Fig. 2B. LPI (0.1-10 μM) produced a dose-dependent increase in $[Ca^{2+}]_i$; with an average amplitude of 9 ± 1.7 nM (n = 105 cells), 73 ± 2.6 nM (n = 94 cells) and 349 ±3.6 nM (n =94- 114 cells) (Fig. 2C). In RBMVEC pretreated with ML-193 (10 μM, 20 min), the effect of LPI (10 μM) was negligible ($\Delta[Ca^{2+}]_i$ = 24 ± 1.7 nM, n = 89 cells, Fig. 2C).

GPR55-mediated Ca^{2+} response is subject to tachyphylaxis

A common feature of the response mediated by G protein-coupled receptors (GPCR) is tachyphylaxis; therefore, we examined the effect of the repetitive application of LPI on the Ca^{2+} response. The first application of LPI (10 μM) elicited a fast and transient increase in $[Ca^{2+}]_i$; the subsequent stimulation with LPI, within 5 minutes of the first stimulation, produced a response with a lower amplitude, suggesting receptor desensitization. A representative example of Ca^{2+} response is shown in Fig. 3A and the comparison of the amplitude ($\Delta[Ca^{2+}]_i$) of the two consecutive responses elicited by LPI in Fig 3B.

LPI promotes Ca^{2+} influx in RBMVEC

The increase in $[Ca^{2+}]_i$ produced by LPI (10 μM) was not affected by pretreatment with U-73122 (10 μM), an inhibitor of phospholipase C (PLC), but was abolished by nifedipine (1 μM), blocker of L-type Ca^{2+} channels, or in Ca^{2+}-free saline (Fig. 4A). Representative examples of increases in $[Ca^{2+}]_i$ produced in each of the conditions mentioned is shown in Fig 4A, and the comparison of the amplitude of the increase in $[Ca^{2+}]_i$ elicited by LPI in the absence/presence of U73122 (10 μM), nifedipine (1 μM) or in Ca^{2+}-free HBSS is shown in Fig. 4B. The mean amplitude of the increase in $[Ca^{2+}]_i$ elicited by LPI was 349 ± 3.6 nM (LPI alone), 344 ± 3.9 nM (in the presence of U-73122), 8 ± 1.8 nM (in the presence of nifedipine) and 12 ± 1.7 nM (in Ca^{2+} free saline); n = 85- 114 cells for each condition.

LPI elicits a biphasic change in membrane potential in RBMVEC

Treatment of RBMVEC with LPI (10 μM) induced a fast and transient depolarization followed by a long-lasting hyperpolarization (Fig. 5A). Pretreatment with ML-193 (10 μM), a GPR55 antagonist, prevented the change in membrane potential induced by LPI. The hyperpolarization elicited by LPI was abolished by treatment with apamin (1 μM) and charibdotoxin (100 nM), inhibitors of small- and intermediate-conductance Ca^{2+}-activated K^+ channels (K_{Ca}), respectively. Averaged recordings of changes in membrane potential in response to LPI, in the absence or presence of ML-193, apamin and charibdotoxin are shown in Fig. 5A, and the comparison of the average amplitude of the hyperpolarization is shown in Fig. 5B. LPI produced a hyperpolarization with a mean amplitude of −5.24 ± 0.31 mV (n = 47 cells); in the presence of ML-193, Δ voltage = − 0.53 ± 0.23 (n = 42 cells); in the presence of apamin and charibdotoxin, Δ voltage = − 0.23 ± 0.31 (n = 39 cells).

LPI alters tight and adherens junctions and cytoskeleton

Immunocytochemistry studies examined the distribution of occludin, a tight junctions protein, ZO-1, an accessory protein that connects the tight junctions proteins to actin cytoskeleton, of VE-cadherin, a component of adherens junctions and of F-actin cytoskeleton (Abbott et al., 2010) before and after GPR55 activation. Treatment with LPI (10 μM) produced a transient disruption of occludin, ZO-1 and VE-cadherin, and formed intercellular gaps, while increasing F-actin stress fiber formation (Fig. 6).

GPR55 activation disrupts endothelial barrier function

Impedance measurements with ECIS method were carried out in RBMVEC monolayers grown on gold electrodes (8W10E+ arrays). Stimulation of confluent monolayers with LPI

(10 μM) produced a fast and transient decrease in electrical resistance measured at 4000 Hz by about 20%, indicating a transient disruption of endothelial barrier function. A typical change in normalized resistance produced by LPI is illustrated in Fig. 7A. Pretreatment of cells on arrays with ML-193 (10 μM, 20 min), reduced the response to LPI (Fig 7A). LPI (1, 3, 5 and 10 μM) produced a dose-dependent reduction in the electrical resistance of RBMVEC monolayer by 1.7 ± 0.3 %, 5.2 ± 0.6 %, 11.4 ± 1.8 % and 19.6 ± 2.4 %, respectively (Fig. 7B). Applying the mathematical model developed by Giaever and Keese (Giaever and Keese, 1991), ECIS experiments indicate that LPI decreased Rb parameter (Fig. 7C), reflecting a transient decrease in tightness of cell-cell junctions (Stolwijk et al., 2015).

LPI increases BBB permeability

In vivo assessment of BBB permeability indicate that in control rats, the brain concentration of Evans Blue was 453 ± 61 ng/mg (n = 6 rats), which was similar to that determined in rat injected with saline or vehicle (DMSO 0.1% v/v, 250 μL) (Fig. 8). Treatment with LPI (10 μM, 250 μL) increased the brain concentration of Evans Blue to 738 ± 136 ng/mg (n = 6 rats). On the other hand, pretreatment with of ML-193 (10 μM, 250 μL) before LPI significantly reduced the Evans Blue concentration in the brain to 582 ± 79 ng/mg (n = 6 rats) (Fig. 8).

Discussion

GPR55 is considered an atypical cannabinoid receptor with a complex and controversial pharmacology (Ross, 2009, Pertwee et al., 2010, Sharir and Abood, 2010, Shore and Reggio, 2015). Lysophosphatidylinositol (LPI) has been identified as the endogenous GPR55 agonist (Oka et al., 2007); the receptor is also activated by endocannabinoids such as anandamide, phytocannabinoids, and synthetic cannabinoid ligands (Zhao and Abood, 2013, Shore and Reggio, 2015). GPR55 has a widespread tissue distribution in the nervous system and peripheral organs and emerging physiologic and pathophysiologic roles (Ryberg et al., 2007, Henstridge et al., 2011, Alhouayek et al., 2018). In the nervous system, GPR55 has been involved in neuronal development, neuroprotection, synaptic transmission, anxiety and pain (Henstridge et al., 2011, Deliu et al., 2015, Guy et al., 2015, Rahimi et al., 2015, Hurst et al., 2017, Alhouayek et al., 2018, Hill et al., 2018).

The blood-brain barrier (BBB) had a critical role in maintaining the brain homeostasis and normal neuronal function (Abbott et al., 2010). Since GPR55 has been identified in human brain endothelial cells (hCMEC/D3) (Hasko et al., 2014, Al Suleimani and Hiley, 2016), we used *in vitro* and *in vivo* studies to examine the role of GPR55 in rat brain microvascular endothelial cells (RBMVEC), an essential component of the BBB.

We first identified the expression of GPR55 at the protein level in RBMVEC. We previously found GPR55 expression in cardiomyoctes (Yu et al., 2013) and neurons from periaqueductal gray, involved in pain processing (Deliu et al., 2015). With respect to endothelial cells, GPR55 was found in microvessels from human dermis (Zhang et al., 2010), lung (Kargl et al., 2013), brain (Hasko et al., 2014) and placenta (Kremshofer et al., 2015). Our earlier studies identified functional GPR55 on both cytosol and plasma

membrane of cardiomyocytes (Yu et al., 2013). We also found that intracellular cannabinoid receptors CB1 (Brailoiu et al., 2011) and CB2 (Brailoiu et al., 2014) are functional. Using immunostaining with a recently characterized GPR55 antibody (Korchynska et al., 2019), GPR55-like immunoreactivity was predominantly detected intracellularly in EBMVEC. Similarly, GPR55 was reported in the cytosol of human neuroblastoma SH-SY5Ycells (Rapino et al., 2019).

We next determined the effect of GPR55 activation on cytosolic Ca^{2+} concentration, $[Ca^{2+}]_i$. Ca^{2+} is a second messenger with a key signaling role in the endothelial cells (Nilius and Droogmans, 2001), that modulates the function of microvascular endothelial cells of the BBB (De Bock et al., 2013). We and others have previously reported that GPR55 activation elicits an increase in $[Ca^{2+}]_i$ in cells endogenously expressing or transfected with the receptor (Oka et al., 2007, Lauckner et al., 2008, Henstridge et al., 2009, Pineiro and Falasca, 2012, Yu et al., 2013, Deliu et al., 2015), including endothelial cells (Bondarenko et al., 2010, AlSuleimani and Hiley, 2015, Al Suleimani and Hiley, 2016). In RBMVEC, LPI (1- 10 μM) produced a fast and transitory increase in $[Ca^{2+}]_i$ in a dose-dependent manner. The concentrations of LPI used in our studies are similar to those previously found to induce a Ca^{2+} response (Bondarenko et al., 2010, Yu et al., 2013, AlSuleimani and Hiley, 2015, Deliu et al., 2015, Al Suleimani and Hiley, 2016, Korchynska et al., 2019).

The LPI-induced rapid and transient Ca^{2+} response in RBMVEC was similar to that reported in human umbilical vein derived endothelial cell line, EA.hy926 (Bondarenko et al., 2010), neurons of periqueductal gray (Deliu et al., 2015), prostate cancer cells (Pineiro and Falasca, 2012) or to the early phase of the Ca^{2+} response produced in endothelial cells of mesenteric arteries (AlSuleimani and Hiley, 2015) or human brain microvascular endothelial cells, hCMEC/D3 (Al Suleimani and Hiley, 2016). LPI, via GPR55 activation, has been also reported to induce different patterns of Ca^{2+} increases: a sustained increase in $[Ca^{2+}]_i$ in neonatal cardiomyocytes (Yu et al., 2013), prolonged, oscillatory Ca^{2+} transients in GPR55-HEK293 cells (Henstridge et al., 2009, Henstridge et al., 2010), or a biphasic Ca^{2+} response (fast and transitory followed by a slow rising sustained increase) in endothelial cells from mesenteric arteries (AlSuleimani and Hiley, 2015) or hCMEC/D3 cells (Al Suleimani and Hiley, 2016). Different patterns of Ca^{2+} increase may be reflective of modulation of different downstream signaling pathways.

One characteristic of GPCR-mediated response is the decrease in response following repetitive or sustained agonist stimulation. We examined the effect of two consecutive applications of LPI on $[Ca^{2+}]_i$; the amplitude of the second response induced by LPI was significantly lower than that of the first response, indicative of tachyphylaxis. This is in agreement with previous studies indicating agonist-induced GPR55 trafficking and internalization (Henstridge et al., 2009, Kapur et al., 2009, Kargl et al., 2013) via beta-arrestin-mediated mechanisms (Kapur et al., 2009).

In endothelial cells, similar to other cell types, an increase in $[Ca^{2+}]_i$ may be produced by Ca^{2+} influx and/or Ca^{2+} release from internal stores (Nilius and Droogmans, 2001). In human umbilical vein EA.hy926 cells, LPI mobilized Ca^{2+} mainly from internal stores (Bondarenko et al., 2010). Similarly, in rat cardiomyocytes (Yu et al., 2013) and

periaqueductal gray neurons (Deliu et al., 2015), LPI released Ca^{2+} from endoplasmic reticulum store via inositol 1,4,5-trisphoshate (IP_3) receptors. A PLC-dependent mechanism was also responsible for LPI-induced increase in $[Ca^{2+}]_i$ in endothelial cells of mesenteric arteries (AlSuleimani and Hiley, 2015) or hCMEC/D3 cells (Al Suleimani and Hiley, 2016). In RBMVEC, the effect of LPI was not affected by U-73122, a PLC inhibitor, but was abolished by inhibiting the voltage-gated L-type Ca^{2+} channels or in Ca^{2+}-free saline indicating that LPI promoted Ca^{2+} influx and not Ca^{2+} release from internal stores in these cells. Previous studies indicate that microvascular endothelial cells, including those from rat brain, are endowed with L-type voltage-gated Ca^{2+} channels (Moccia et al., 2012). Our results indicate that in RBMVEC, GPR55 activation promotes Ca^{2+} influx and does not involve PLC-mediated signaling. In smooth muscle cells of rat coronary artery, LPI induced Ca^{2+} influx via store-operated calcium entry (Smani et al., 2007).

Earlier reports indicate that LPI modulates the membrane potential of endothelial cells (Bondarenko et al., 2010) or neurons (Deliu et al., 2015). In RBMVEC, LPI induced a fast and transient depolarization followed by a long-lasting hyperpolarization. The change in membrane potential induced by LPI was prevented by ML-193, a GPR55 antagonist, indicating that it was mediated by this receptor. Endothelial hyperpolarization is mediated by activation of small- and intermediate-conductance Ca^{2+}-activated K^+ channels (SK_{Ca} and IK_{Ca}) (Gluais et al., 2005, Feletou, 2009). In RBMVEC, LPI-induced hyperpolarization phase was abolished by blocking SK_{Ca} and IK_{Ca} with apamin and charibdotoxin, respectively. Similarly, previous studies indicate that human umbilical vein derived endothelial cell line EA.hy926 (Bondarenko et al., 2010, Bondarenko et al., 2011) or in human pulmonary arteries (Karpinska et al., 2018) LPI activates K_{Ca}. However, in EA.hy926 cells, the sequence of changes in membrane potential following LPI treatment was reversed: the initial hyperpolarization, mediated by activation of K_{Ca} conductance was followed by a long-lasting depolarization via activation of non-selective cation channels and inhibition of Na^+/K^+ ATP-ase (Bondarenko et al., 2010). Moreover, in EA.hy926 cells, the hyperpolarization, but not the depolarization phase was sensitive to rimonabant (Bondarenko et al., 2010), a GPR55 antagonist (Lauckner et al., 2008), indicating a GPR55-independent mechanism for the depolarization. The differences reported in the membrane potential change induced by LPI in RBMVEC versus EA.hy926 cells may indicate different signaling mechanisms employed by GPR55 activation in primary endothelial cells versus endothelial cell lines.

Microvascular endothelial cells of the BBB form a tight monolayer with high endothelial electrical resistance and low paracellular permeability, connected via tight and adherens junctions (Abbott et al., 2010). Tight junctions consists of a complex network of transmembrane proteins including occludin, claudin and junctional adhesion molecules spanning between the cells, connected via zona occludens cytoplasmic regulatory proteins such as ZO-1 with actin filaments (Cardoso et al., 2010). Adherens junctions comprise of VE-cadherin connected via cytoplasmic catenins with actin cytoskeleton (Cardoso et al., 2010). Tight and adherens junctions are highly dynamic structures (Huber et al., 2001, Cardoso et al., 2010). Dissociation of tight/adherens junctions and reorganization of actin cytoskeleton leads to disruption of barrier function and increase in permeability (Stolwijk et al., 2016). Our results indicate that in RBMVEC, LPI via GPR55 activation produced a

transient reorganization of occludin and ZO-1, components of tight junctions, and of VE-cadherin, an adherens junction protein. In addition, LPI produced redistribution of F-actin fibers and formation of intercellular gaps. Barrier-disrupting agonists such as platelet-activating factor (Brailoiu et al., 2018), histamine or thrombin (Stolwijk et al., 2016, Brailoiu et al., 2017) produced similar changes in tight and adherens junctions proteins and F-actin in microvascular endothelial cells, but the effect of LPI was shorter-lasting.

The transient changes in junctional proteins and cytoskeleton immunoreactivity elicited by GPR55 activation in RBMVEC can be consequent to the LPI-induced increase in $[Ca^{2+}]_i$. Extracellular and cytosolic Ca^{2+} concentration play a critical role in BBB function; an increase in $[Ca^{2+}]_i$ has been associated with reorganization of junctional and cytoskeletal proteins and an increase in BBB permeability (Tiruppathi et al., 2006, De Bock et al., 2013). Activation of Ca^{2+}/calmodulin-dependent MLCK by Ca^{2+} leads to MLC phosphorylation, actin-myosin cross-bridge formation, disassembly of VE-cadherin junctions, weakening of junctions and intercellular gap formation, leading to an increase in paracellular permeability (De Bock et al., 2013). Ca^{2+}-dependent phosphorylation of tight junction proteins, occludin and ZO-1, can also produce a decrease in transendothelial resistance and increased permeability (Huber et al., 2001).

The morphological changes induced by LPI were consistent with the transient reduction in the electrical resistance of RBMVEC monolayer assessed via ECIS. In addition to the evaluation of the magnitude of resistance decrease, ECIS allows the investigation of the kinetics of barrier breakdown and recovery (Stolwijk et al., 2015). The electrical resistance at low frequency (4000 Hz) reflects the functional characteristics and stability of the cell-cell tight and adherens junctions. Moreover, our ECIS analysis, applying mathematical modeling (Giaever and Keese, 1991) indicates that LPI produced a reduction in the Rb parameter, that measures the electrical resistance in the intercellular cleft, determined by the tightness of the monolayer. A decrease in Rb reflects an increase in paracellular permeability. Similarly, LPI has been reported to reduce the resistance and the integrity of human umbilical vein endothelial cells HUVEC monolayer (Kargl et al., 2016).

We investigated the *in vivo* functional significance of our *in vitro* findings by assessing the effect of systemic administration of LPI on the BBB permeability. LPI administration increased Evans Blue accumulation in the brain, indicating an increase in BBB permeability. Our results indicate that in addition to previously reported neuronal effects, LPI acting on GPR55 modulates directly the function of brain microvessels and produces a transient decrease in endothelial barrier function and an increase in the BBB permeability.

Acknowledgements

Research reported in this publication was supported by funds from the Jefferson College of Pharmacy, the National Institute of Neurological Disorders and Stroke of the National Institutes of Health (NIH) under Award Number R03NS099957, and by NIH grants R01 DA035926, T32 DA007237 and P30 DA 013429. We are grateful to Ken Mackie (Indiana University, Bloomington, IN) for providing GPR55 antibody and immunizing peptide for immunocytochemistry studies.

Abbreviations:

BBB	blood-brain barrier
$[Ca^{2+}]_i$	cytosolic Ca^{2+} concentration
ECIS	Electric Cell-Substrate Impedance Sensing
HBSS	Hanks Balanced Salt Solution
LPI	lysophosphatidylinositol
PLC	phospholipase C
RBMVEC	rat brain microvascular endothelial cells
ZO-1	zona occludens-1

References

Abbott NJ, Patabendige AA, Dolman DE, Yusof SR, Begley DJ (2010) Structure and function of the blood-brain barrier. Neurobiology of disease 37:13–25. [PubMed: 19664713]

Al Suleimani YM, Hiley CR (2016) Characterization of calcium signals provoked by lysophosphatidylinositol in human microvascular endothelial cells. Physiological research 65:53–62. [PubMed: 26596318]

Alhouayek M, Masquelier J, Muccioli GG (2018) Lysophosphatidylinositols, from Cell Membrane Constituents to GPR55 Ligands. Trends in pharmacological sciences 39:586–604. [PubMed: 29588059]

AlSuleimani YM, Hiley CR (2015) The GPR55 agonist lysophosphatidylinositol relaxes rat mesenteric resistance artery and induces Ca(2+) release in rat mesenteric artery endothelial cells. British journal of pharmacology 172:3043–3057. [PubMed: 25652040]

Altmann JB, Yan G, Meeks JF, Abood ME, Brailoiu E, Brailoiu GC (2015) G protein-coupled estrogen receptor-mediated effects on cytosolic calcium and nanomechanics in brain microvascular endothelial cells. Journal of neurochemistry 133:629–639. [PubMed: 25703621]

Baker D, Pryce G, Davies WL, Hiley CR (2006) In silico patent searching reveals a new cannabinoid receptor. Trends in pharmacological sciences 27:1–4. [PubMed: 16318877]

Bondarenko A, Waldeck-Weiermair M, Naghdi S, Poteser M, Malli R, Graier WF (2010) GPR55-dependent and -independent ion signalling in response to lysophosphatidylinositol in endothelial cells. British journal of pharmacology 161:308–320. [PubMed: 20735417]

Bondarenko AI, Malli R, Graier WF (2011) The GPR55 agonist lysophosphatidylinositol directly activates intermediate-conductance Ca2+ -activated K+ channels. Pflugers Archiv : European journal of physiology 462:245–255. [PubMed: 21603896]

Brailoiu E, Barlow CL, Ramirez SH, Abood ME, Brailoiu GC (2018) Effects of Platelet-Activating Factor on Brain Microvascular Endothelial Cells. Neuroscience 377:105–113. [PubMed: 29522856]

Brailoiu E, Shipsky MM, Yan G, Abood ME, Brailoiu GC (2017) Mechanisms of modulation of brain microvascular endothelial cells function by thrombin. Brain research 1657:167–175. [PubMed: 27998795]

Brailoiu GC, Deliu E, Console-Bram LM, Soboloff J, Abood ME, Unterwald EM, Brailoiu E (2016) Cocaine inhibits store-operated Ca2+ entry in brain microvascular endothelial cells: critical role for sigma-1 receptors. The Biochemical journal 473:1–5. [PubMed: 26467159]

Brailoiu GC, Deliu E, Marcu J, Hoffman NE, Console-Bram L, Zhao P, Madesh M, Abood ME, Brailoiu E (2014) Differential activation of intracellular versus plasmalemmal CB2 cannabinoid receptors. Biochemistry 53:4990–4999. [PubMed: 25033246]

Brailoiu GC, Oprea TI, Zhao P, Abood ME, Brailoiu E (2011) Intracellular cannabinoid type 1 (CB1) receptors are activated by anandamide. J Biol Chem 286:29166–29174. [PubMed: 21719698]

Brauner T, Hulser DF, Strasser RJ (1984) Comparative measurements of membrane potentials with microelectrodes and voltage-sensitive dyes. Biochimica et biophysica acta 771:208–216. [PubMed: 6704395]

Cardoso FL, Brites D, Brito MA (2010) Looking at the blood-brain barrier: molecular anatomy and possible investigation approaches. Brain research reviews 64:328–363. [PubMed: 20685221]

De Bock M, Wang N, Decrock E, Bol M, Gadicherla AK, Culot M, Cecchelli R, Bultynck G, Leybaert L (2013) Endothelial calcium dynamics, connexin channels and blood-brain barrier function. Progress in neurobiology 108:1–20. [PubMed: 23851106]

Deliu E, Sperow M, Console-Bram L, Carter RL, Tilley DG, Kalamarides DJ, Kirby LG, Brailoiu GC, Brailoiu E, Benamar K, Abood ME (2015) The Lysophosphatidylinositol Receptor GPR55 Modulates Pain Perception in the Periaqueductal Gray. Molecular pharmacology 88:265–272. [PubMed: 25972448]

Feletou M (2009) Calcium-activated potassium channels and endothelial dysfunction: therapeutic options? British journal of pharmacology 156:545–562. [PubMed: 19187341]

Ferro R, Adamska A, Lattanzio R, Mavrommati I, Edling CE, Arifin SA, Fyffe CA, Sala G, Sacchetto L, Chiorino G, De Laurenzi V, Piantelli M, Sansom OJ, Maffucci T, Falasca M (2018) GPR55 signalling promotes proliferation of pancreatic cancer cells and tumour growth in mice, and its inhibition increases effects of gemcitabine. Oncogene.

Giaever I, Keese CR (1984) Monitoring fibroblast behavior in tissue culture with an applied electric field. Proc Natl Acad Sci U S A 81:3761–3764. [PubMed: 6587391]

Giaever I, Keese CR (1991) Micromotion of mammalian cells measured electrically. Proc Natl Acad Sci U S A 88:7896–7900. [PubMed: 1881923]

Gluais P, Edwards G, Weston AH, Falck JR, Vanhoutte PM, Feletou M (2005) Role of SK(Ca) and IK(Ca) in endothelium-dependent hyperpolarizations of the guinea-pig isolated carotid artery. British journal of pharmacology 144:477–485. [PubMed: 15655533]

Grynkiewicz G, Poenie M, Tsien RY (1985) A new generation of Ca2+ indicators with greatly improved fluorescence properties. J Biol Chem 260:3440–3450. [PubMed: 3838314]

Guy AT, Nagatsuka Y, Ooashi N, Inoue M, Nakata A, Greimel P, Inoue A, Nabetani T, Murayama A, Ohta K, Ito Y, Aoki J, Hirabayashi Y, Kamiguchi H (2015) NEURONAL DEVELOPMENT. Glycerophospholipid regulation of modality-specific sensory axon guidance in the spinal cord. Science 349:974–977. [PubMed: 26315437]

Hasko J, Fazakas C, Molnar J, Nyul-Toth A, Herman H, Hermenean A, Wilhelm I, Persidsky Y, Krizbai IA (2014) CB2 receptor activation inhibits melanoma cell transmigration through the blood-brain barrier. International journal of molecular sciences 15:8063–8074. [PubMed: 24815068]

Henstridge CM, Balenga NA, Ford LA, Ross RA, Waldhoer M, Irving AJ (2009) The GPR55 ligand L-alpha-lysophosphatidylinositol promotes RhoA-dependent Ca2+ signaling and NFAT activation. FASEB journal : official publication of the Federation of American Societies for Experimental Biology 23:183–193. [PubMed: 18757503]

Henstridge CM, Balenga NA, Kargl J, Andradas C, Brown AJ, Irving A, Sanchez C, Waldhoer M (2011) Minireview: recent developments in the physiology and pathology of the lysophosphatidylinositol-sensitive receptor GPR55. Molecular endocrinology 25:1835–1848. [PubMed: 21964594]

Henstridge CM, Balenga NA, Schroder R, Kargl JK, Platzer W, Martini L, Arthur S, Penman J, Whistler JL, Kostenis E, Waldhoer M, Irving AJ (2010) GPR55 ligands promote receptor coupling to multiple signalling pathways. British journal of pharmacology 160:604–614. [PubMed: 20136841]

Heynen-Genel S, Dahl R, Shi S, Milan L, Hariharan S, Sergienko E, Hedrick M, Dad S, Stonich D, Su Y, Vicchiarelli M, Mangravita-Novo A, Smith LH, Chung TDY, Sharir H, Caron MG, Barak LS, Abood ME (2010b) Screening for Selective Ligands for GPR55 - Antagonists. Probe Reports from the NIH Molecular Libraries Program [Internet]

Hill JD, Zuluaga-Ramirez V, Gajghate S, Winfield M, Persidsky Y (2018) Activation of GPR55 increases neural stem cell proliferation and promotes early adult hippocampal neurogenesis. British journal of pharmacology.

Huber JD, Egleton RD, Davis TP (2001) Molecular physiology and pathophysiology of tight junctions in the blood-brain barrier. Trends in neurosciences 24:719–725. [PubMed: 11718877]

Hurst K, Badgley C, Ellsworth T, Bell S, Friend L, Prince B, Welch J, Cowan Z, Williamson R, Lyon C, Anderson B, Poole B, Christensen M, McNeil M, Call J, Edwards JG (2017) A putative lysophosphatidylinositol receptor GPR55 modulates hippocampal synaptic plasticity. Hippocampus 27:985–998. [PubMed: 28653801]

Kapur A, Zhao P, Sharir H, Bai Y, Caron MG, Barak LS, Abood ME (2009) Atypical responsiveness of the orphan receptor GPR55 to cannabinoid ligands. J Biol Chem 284:29817–29827. [PubMed: 19723626]

Kargl J, Andersen L, Hasenohrl C, Feuersinger D, Stancic A, Fauland A, Magnes C, El-Heliebi A, Lax S, Uranitsch S, Haybaeck J, Heinemann A, Schicho R (2016) GPR55 promotes migration and adhesion of colon cancer cells indicating a role in metastasis. British journal of pharmacology 173:142–154. [PubMed: 26436760]

Kargl J, Brown AJ, Andersen L, Dorn G, Schicho R, Waldhoer M, Heinemann A (2013) A selective antagonist reveals a potential role of G protein-coupled receptor 55 in platelet and endothelial cell function. The Journal of pharmacology and experimental therapeutics 346:54–66. [PubMed: 23639801]

Karpinska O, Baranowska-Kuczko M, Malinowska B, Kloza M, Kusaczuk M, Gegotek A, Golec P, Kasacka I, Kozlowska H (2018) Mechanisms of l-alpha-lysophosphatidylinositol-induced relaxation in human pulmonary arteries. Life sciences 192:38–45. [PubMed: 29155298]

Korchynska S, Lutz MI, Borok E, Pammer J, Cinquina V, Fedirko N, Irving AJ, Mackie K, Harkany T, Keimpema E (2019) GPR55 controls functional differentiation of self-renewing epithelial progenitors for salivation. JCI insight 4.

Kotsikorou E, Sharir H, Shore DM, Hurst DP, Lynch DL, Madrigal KE, Heynen-Genel S, Milan LB, Chung TD, Seltzman HH, Bai Y, Caron MG, Barak LS, Croatt MP, Abood ME, Reggio PH (2013) Identification of the GPR55 antagonist binding site using a novel set of high-potency GPR55 selective ligands. Biochemistry 52:9456–9469. [PubMed: 24274581]

Kremshofer J, Siwetz M, Berghold VM, Lang I, Huppertz B, Gauster M (2015) A role for GPR55 in human placental venous endothelial cells. Histochemistry and cell biology 144:49–58. [PubMed: 25869640]

Lauckner JE, Jensen JB, Chen HY, Lu HC, Hille B, Mackie K (2008) GPR55 is a cannabinoid receptor that increases intracellular calcium and inhibits M current. Proc Natl Acad Sci U S A 105:2699–2704. [PubMed: 18263732]

Martin TW, Wysolmerski RB (1987) Ca2+-dependent and Ca2+-independent pathways for release of arachidonic acid from phosphatidylinositol in endothelial cells. J Biol Chem 262:13086–13092. [PubMed: 3115976]

Moccia F, Berra-Romani R, Tanzi F (2012) Update on vascular endothelial Ca(2+) signalling: A tale of ion channels, pumps and transporters. World journal of biological chemistry 3:127–158. [PubMed: 22905291]

Nilius B, Droogmans G (2001) Ion channels and their functional role in vascular endothelium. Physiological reviews 81:1415–1459. [PubMed: 11581493]

Oka S, Nakajima K, Yamashita A, Kishimoto S, Sugiura T (2007) Identification of GPR55 as a lysophosphatidylinositol receptor. Biochemical and biophysical research communications 362:928–934. [PubMed: 17765871]

Pertwee RG, Howlett AC, Abood ME, Alexander SP, Di Marzo V, Elphick MR, Greasley PJ, Hansen HS, Kunos G, Mackie K, Mechoulam R, Ross RA (2010) International Union of Basic and Clinical Pharmacology. LXXIX. Cannabinoid receptors and their ligands: beyond CB1 and CB2. Pharmacol Rev 62:588–631. [PubMed: 21079038]

Pineiro R, Falasca M (2012) Lysophosphatidylinositol signalling: new wine from an old bottle. Biochimica et biophysica acta 1821:694–705. [PubMed: 22285325]

Pineiro R, Maffucci T, Falasca M (2011) The putative cannabinoid receptor GPR55 defines a novel autocrine loop in cancer cell proliferation. Oncogene 30:142–152. [PubMed: 20838378]

Rahimi A, Hajizadeh Moghaddam A, Roohbakhsh A (2015) Central administration of GPR55 receptor agonist and antagonist modulates anxiety-related behaviors in rats. Fundamental & clinical pharmacology 29:185–190. [PubMed: 25620584]

Rapino C, Castellucci A, Lizzi AR, Sabatucci A, Angelucci CB, Tortolani D, Rossi G, D'Andrea G, Maccarrone M (2019) Modulation of Endocannabinoid-Binding Receptors in Human Neuroblastoma Cells by Tunicamycin. Molecules 24.

Ross RA (2009) The enigmatic pharmacology of GPR55. Trends in pharmacological sciences 30:156–163. [PubMed: 19233486]

Ross RA (2011) L-alpha-lysophosphatidylinositol meets GPR55: a deadly relationship. Trends in pharmacological sciences 32:265–269. [PubMed: 21367464]

Ryberg E, Larsson N, Sjogren S, Hjorth S, Hermansson NO, Leonova J, Elebring T, Nilsson K, Drmota T, Greasley PJ (2007) The orphan receptor GPR55 is a novel cannabinoid receptor. British journal of pharmacology 152:1092–1101. [PubMed: 17876302]

Sharir H, Abood ME (2010) Pharmacological characterization of GPR55, a putative cannabinoid receptor. Pharmacol Ther 126:301–313. [PubMed: 20298715]

Shore DM, Reggio PH (2015) The therapeutic potential of orphan GPCRs, GPR35 and GPR55. Frontiers in pharmacology 6:69. [PubMed: 25926795]

Smani T, Dominguez-Rodriguez A, Hmadcha A, Calderon-Sanchez E, Horrillo-Ledesma A, Ordonez A (2007) Role of Ca2+-independent phospholipase A2 and store-operated pathway in urocortin-induced vasodilatation of rat coronary artery. Circulation research 101:1194–1203. [PubMed: 17885217]

Stolwijk JA, Matrougui K, Renken CW, Trebak M (2015) Impedance analysis of GPCR-mediated changes in endothelial barrier function: overview and fundamental considerations for stable and reproducible measurements. Pflugers Archiv : European journal of physiology 467:2193–2218. [PubMed: 25537398]

Stolwijk JA, Zhang X, Gueguinou M, Zhang W, Matrougui K, Renken C, Trebak M (2016) Calcium Signaling Is Dispensable for Receptor Regulation of Endothelial Barrier Function. The Journal of biological chemistry 291:22894–22912. [PubMed: 27624938]

Tiruppathi C, Ahmmed GU, Vogel SM, Malik AB (2006) Ca2+ signaling, TRP channels, and endothelial permeability. Microcirculation 13:693–708. [PubMed: 17085428]

Uyama O, Okamura N, Yanase M, Narita M, Kawabata K, Sugita M (1988) Quantitative evaluation of vascular permeability in the gerbil brain after transient ischemia using Evans blue fluorescence. Journal of cerebral blood flow and metabolism : official journal of the International Society of Cerebral Blood Flow and Metabolism 8:282–284.

Yu J, Deliu E, Zhang XQ, Hoffman NE, Carter RL, Grisanti LA, Brailoiu GC, Madesh M, Cheung JY, Force T, Abood ME, Koch WJ, Tilley DG, Brailoiu E (2013) Differential activation of cultured neonatal cardiomyocytes by plasmalemmal versus intracellular G protein-coupled receptor 55. J Biol Chem 288:22481–22492. [PubMed: 23814062]

Zhang X, Maor Y, Wang JF, Kunos G, Groopman JE (2010) Endocannabinoid-like N-arachidonoyl serine is a novel pro-angiogenic mediator. British journal of pharmacology 160:1583–1594. [PubMed: 20649563]

Zhao P, Abood ME (2013) GPR55 and GPR35 and their relationship to cannabinoid and lysophospholipid receptors. Life sciences 92:453–457. [PubMed: 22820167]

Highlights

- GPR55, atypical cannabinoid receptor activated by LPI, is expressed in rat brain microvascular endothelial cells (RBMVEC)
- In RBMVC, LPI increased cytosolic Ca^{2+} and produced a fast depolarization followed by a long-lasting hyperpolarization.
- LPI disrupted tight and adherens junctions proteins and altered RBMVEC barrier function assessed with ECIS.
- *In vivo* studies, reveal for the first time that LPI via GPR55 activation increases BBB permeability.

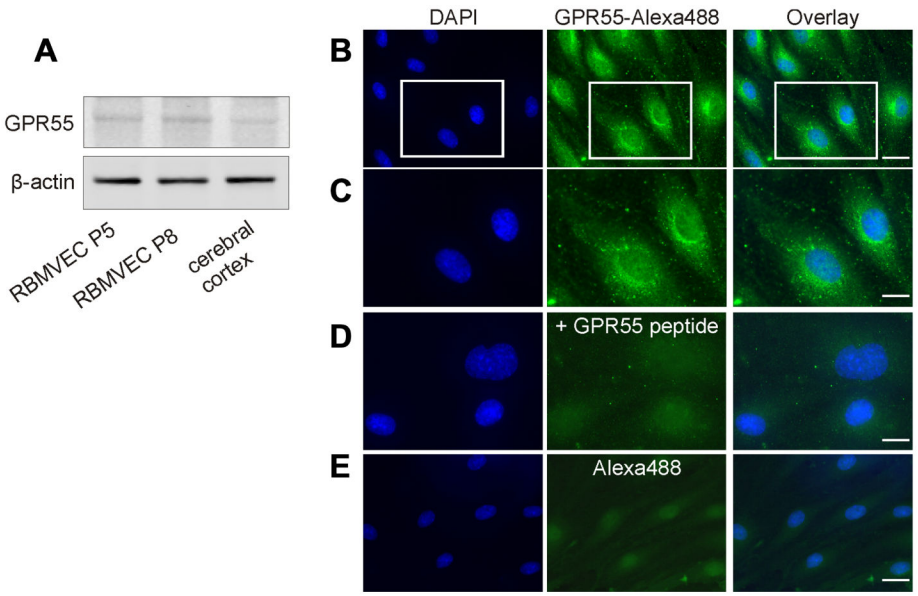

Fig. 1. GPR55 expression and distribution in rat brain microvascular endothelial cells (RBMVEC).

A, Western blot analysis of RBMVEC passage 5 (P5), passage 8 (P8) and rat cerebral cortex indicates the presence of GPR55 at the protein level; β-actin was used as an internal loading control. **B.** GPR55-like immunoreactivity was found mostly intracellularly; scarce GPR55-like immunoreactivity was seen at the plasma membrane; nuclei are stained with DAPI. **C**, Higher magnification image of the area outlined in B, illustrating the cellular distribution of GPR55 immunoreactivity. **D**. Example of control experiments, where GPR55 antibody was incubated with the immunizing peptide; a low basal fluorescence level was detected using Alexa Fluor 488 secondary antibodies. **E**. Example of control experiments, where GPR55 antibody was omitted, indicating low background fluorescence detected with the secondary antibody Alexa Fluor 488. Scale bar, 20 μm in B and E; 10 μm in C and D.

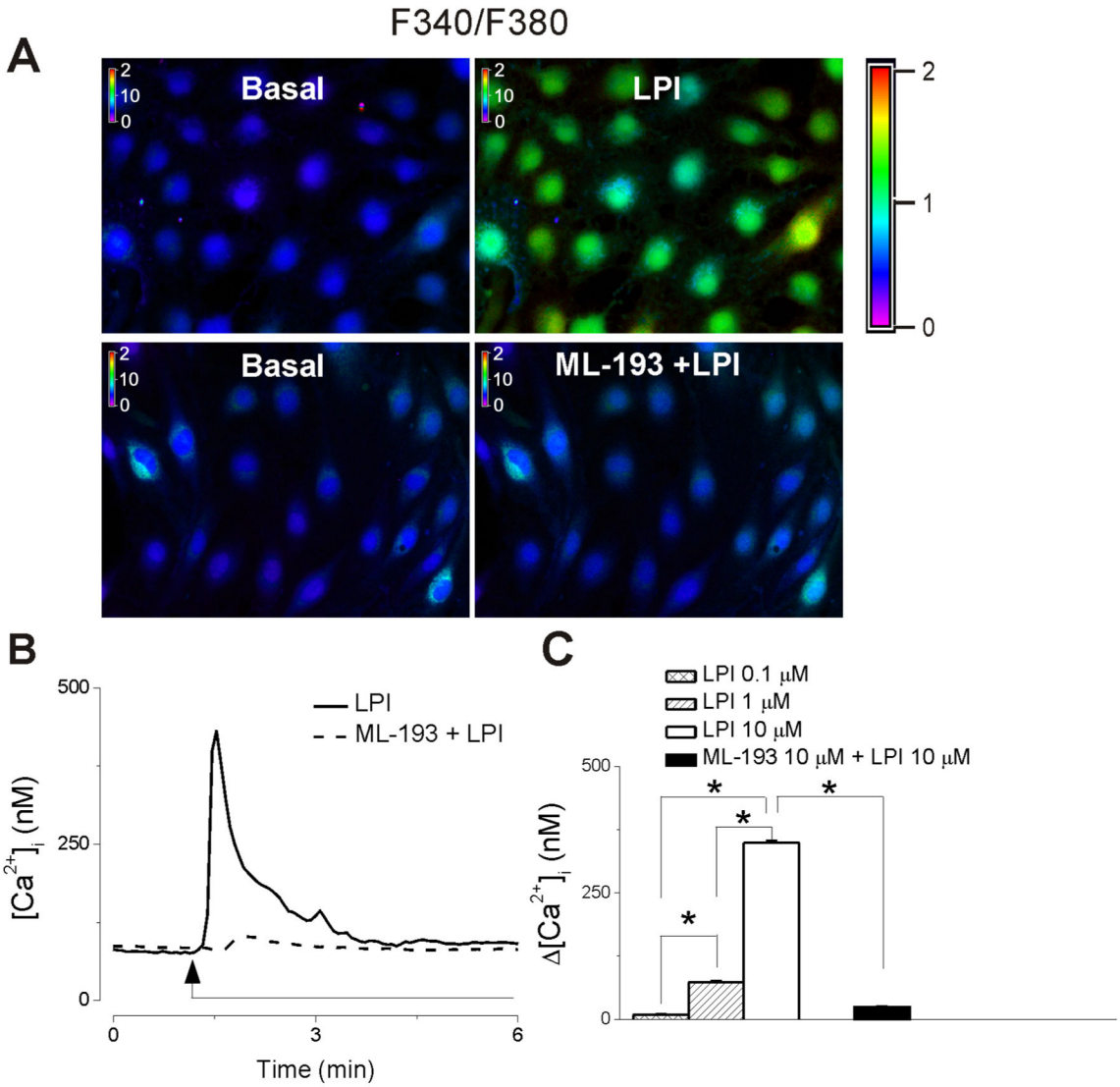

Fig. 2. GPR55 activation in RBMVEC increases cytosolic Ca^{2+} concentration, $[Ca^{2+}]_i$.

A, Example of increases in F340/F380 fluorescence ratio in RBMVEC produced by LPI (10 μM), the GPR55 agonist; the response was prevented by ML-193 (10 μM), a GPR55 antagonist. **B**, LPI (10 μM) produced a fast and transitory increase in cytosolic Ca^{2+} concentration, $[Ca^{2+}]_i$ (solid trace), ML-193 abolished the response to LPI (dashed trace). **C**, Comparison of the average amplitude ± SEM of the increase in $[Ca^{2+}]_i$ produced by different concentrations of LPI, and LPI in cells pretreated with ML-193. LPI (0.1, 1 and 10 μM) produced a dose-dependent increase in $[Ca^{2+}]_i$ (*$P < 0.05$).

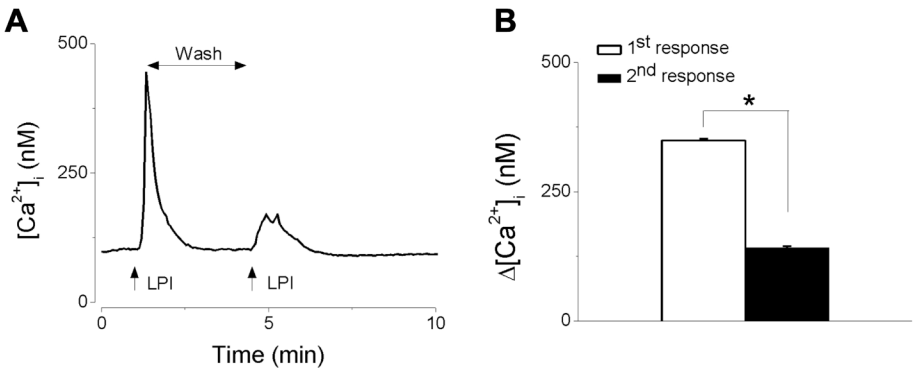

Fig. 3. Repetitive application of LPI leads to tachyphylaxis.

A, Representative example of increases in $[Ca^{2+}]_i$, produced by two consecutive applications of LPI (10 μM) indicating that the second response has a smaller amplitude. **B**. Comparison of the amplitude of the increase in $[Ca^{2+}]_i$, produced by two consecutive applications of LPI (10 μM) (*$P < 0.05$).

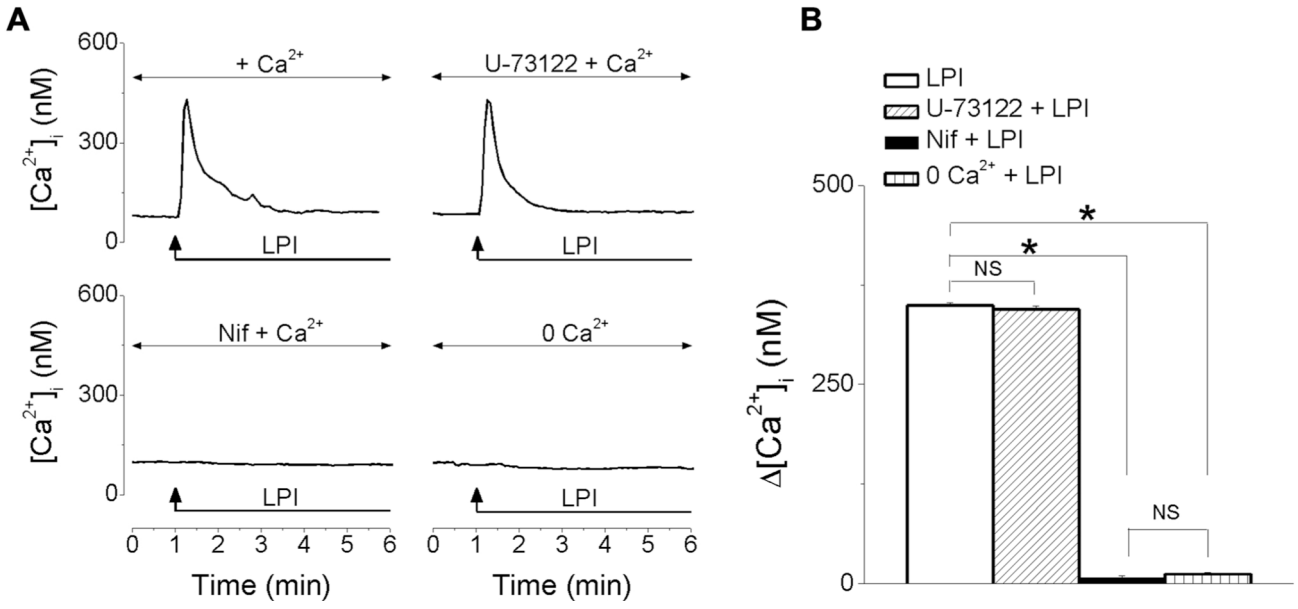

Fig. 4. LPI promotes Ca^{2+} influx in RBMVEC.

A, Representative examples of increases in $[Ca^{2+}]_i$ produced by LPI in the absence/presence of the PLC inhibitor, U-73122 (10 μM), of L-type Ca^{2+} channel blocker, nifedipine (1 μM), and in Ca^{2+}-free saline. **B,** Comparison of the amplitude of the average increase in $[Ca^{2+}]_i$ elicited by LPI in each of the conditions mentioned; U-73122 did not affect the amplitude of LPI-induced increase in $[Ca^{2+}]_i$, while nifedipine or Ca^{2+}-free saline abolished the response to LPI. (*$P < 0.05$; NS – not significant).

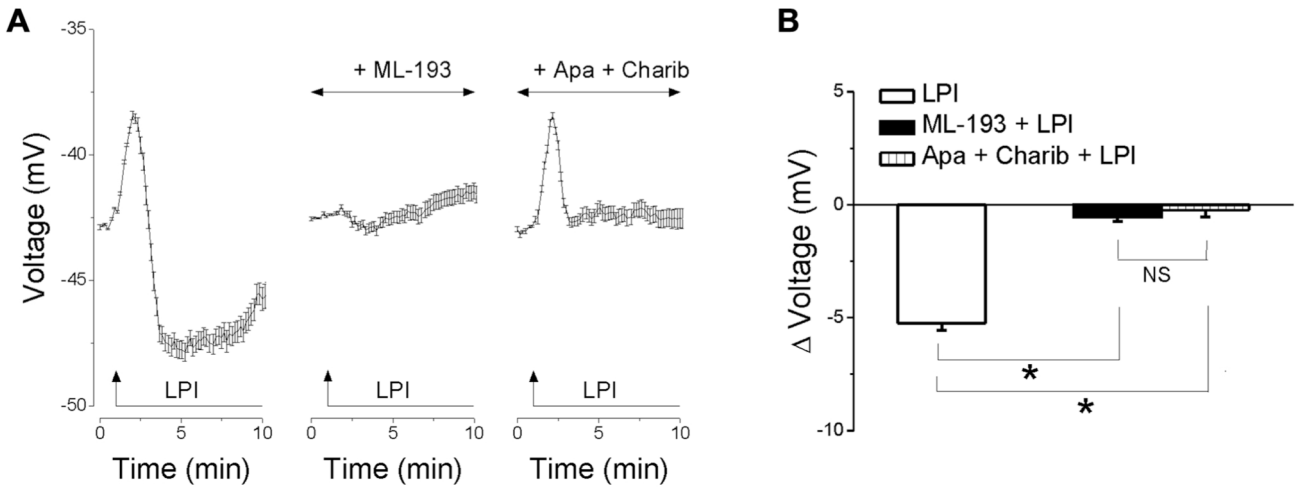

Fig. 5. LPI elicits a biphasic change in membrane potential in RBMVEC.

A, Averaged changes in membrane potential ± SEM. in response to LPI (10 μM) in the absence or presence of the GPR55 antagonist, ML-193 (10 μM), or of inhibitors of small- and intermediate-conductance Ca^{2+}-activated K^+ channels (K_{Ca}), apamin (1 μM), and charibdotoxin (100 nM). Treatment of RBMVEC with LPI (10 μM) induced a fast and transient depolarization followed by a long-lasting hyperpolarization. The response to LPI was prevented by ML-193; the hyperpolarization phase was sensitive to apamin and charibdotoxin. **B**, Comparison of the average amplitude ± SEM of the hyperpolarization produced by LPI in the absence and presence of ML-193 and of apamin and charibdotoxin. (*$P < 0.05$; NS – not significant).

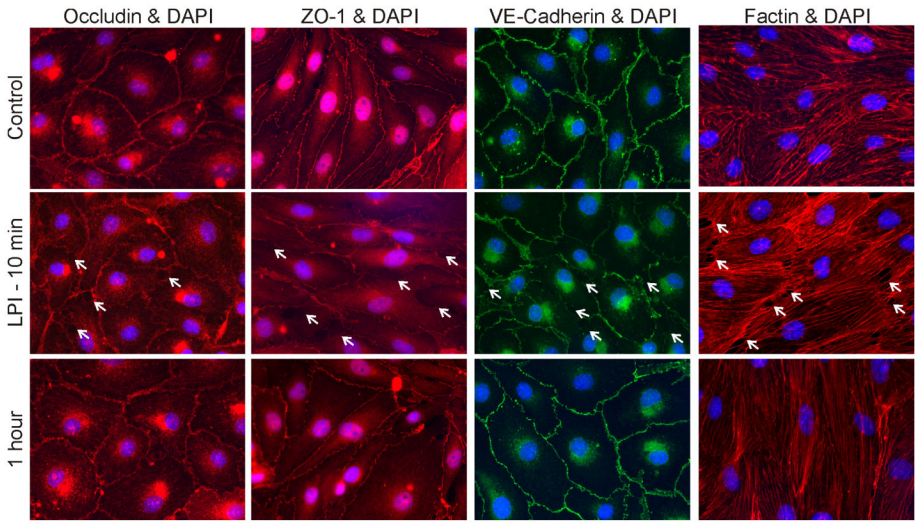

Fig. 6. LPI produced transient changes in tight and adherens junctions proteins and F-actin.

Distribution of tight junction protein occludin, accessory protein ZO-1, adherens junction protein VE-cadherin and F-actin, a component of cytoskeleton, in control RBMVEC, and cells treated with LPI (10 μM) for 10 min, and one hour after LPI treatment. Nuclei are stained with DAPI. Treatment with LPI produced a transient disruption of immunoreactivity for occludin, ZO-1, VE-cadherin, reorganization of actin fibers, and formation of intercellular gaps (arrows).

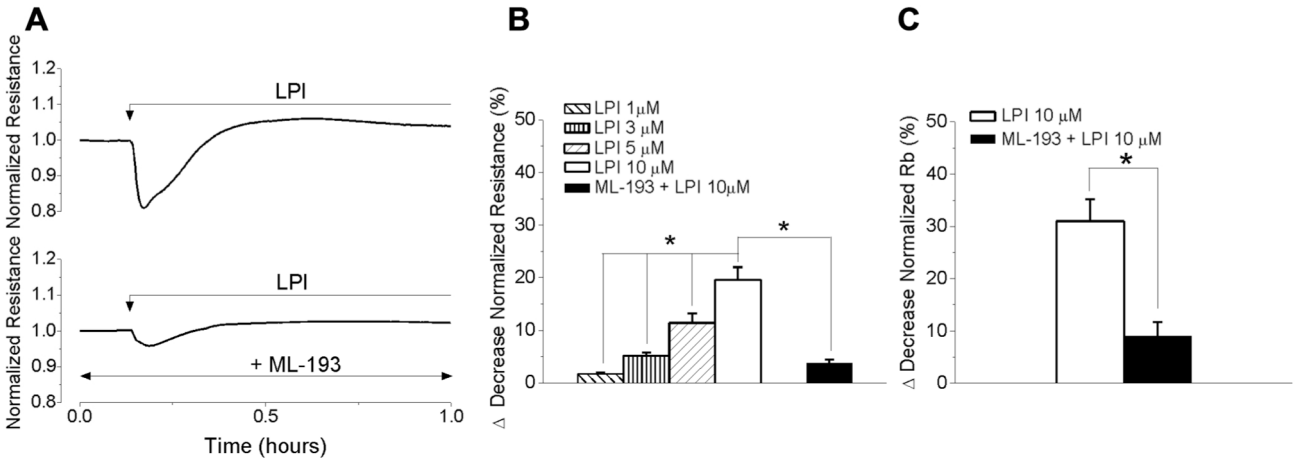

Fig. 7. LPI produced a transient disruption of RBMVEC barrier function.

A, LPI (10 μM) produced a transient decrease in the normalized resistance (measured at 4000 Hz) of confluent RBMVEC monolayer assessed with Electric Cell-Substrate Impedance Sensing (ECIS); the response was reduced by pretreatment with ML-193. **B**, Comparison of the decrease in normalized resistance of RBMVEC monolayer produced by LPI (1-10 μM) and ML-193 + LPI. **C**, Comparison of the decrease (%) in normalized Rb parameter, that reflects the resistance in the intercellular cleft (*$P < 0.05$).

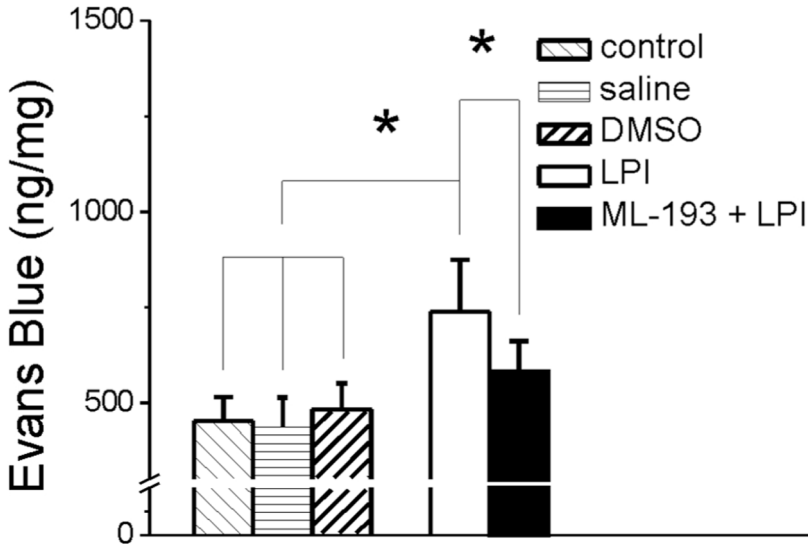

Fig. 8. LPI increased the permeability of the blood-brain barrier (BBB) *in vivo*.

Systemic (i.v.) administration of LPI increased the BBB permeability assessed using the Evans Blue method; the effect was reduced by treatment with ML-193. Brain Evans Blue concentration after injection of saline or DMSO (0.1% v/v) was not significantly different from control rats; $*P < 0.05$.

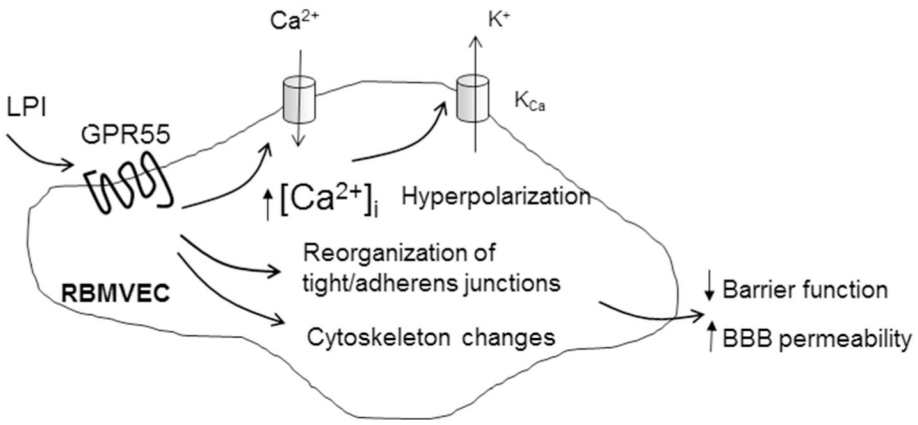

Fig. 9. Diagram summarizing the effect of LPI on RBMVEC.

LPI via GPR55 activation increases cytosolic Ca^{2+} concentration, $[Ca^{2+}]_i$, by promoting Ca^{2+} influx through L-type voltage-gated Ca^{2+} channels, activates Ca^{2+}-dependent K^+ channels leading to hyperpolarization. LPI produces disruption of tight and adherens junctions, and reorganization of F-actin stress fibers leading to a transient reduction in endothelial barrier function and increased BBB permeability.